GEOPHYSICAL RESEARCH LETTER, VOL. 20, NO. 8, PAGES 647-650, APRIL 23, 1993

A RUPTURE MODEL FOR THE 28 JUNE 1992 LANDERS, CALIFORNIA, EARTHQUAKE

MICHEL CAMPILLO
LGIT/IRIGM, Université Joseph Fourier, Grenoble, France

RALPH J. ARCHULETA
Institute for Crustal Studies and Department of Geological Sciences
University of California, Santa Barbara, California

Abstract. We have modeled displacement time histories to infer the large-scale rupture process of the 28 June 1992 M 7.4 Landers, California, earthquake. We have used integrated accelerograms from four TERRAscope stations at distances between 70 and 150 km. The earthquake process consists of unilateral rupture propagation, 3 km/s, on two distinct segments with different strikes: N10°W and N40°W. The two segments are 20 and 30 km long with constant slip of 3.5 m and 5.2 m, respectively. The excitation of surface waves, resulting from a low-velocity surficial layer, plays a critical role in matching the synthetic waveforms to the observed displacements. The displacements, due to both body waves and surface waves, are strongly affected by directivity. Matching the synthetics to the data requires a one second delay between the end of rupture on the first segment and the initiation of rupture on the second segment. The seismic moment of the subevents are 2.8×10^{19} N-m and 8.4×10^{19} N-m, leading to a total moment of 1.12×10^{20} N-m (M=7.4).

INTRODUCTION

The M 7.4 Landers, California, earthquake of 28 June 1992 severely shook the Mojave Desert area and produced the largest surface offsets in California since the great 1857 Southern California earthquake. Figure 1 shows a map of the rupture breaks together with the location of the epicenter of the Landers' earthquake. Figure 1 also shows the epicenters of aftershocks including the M_L 6.5 Big Bear earthquake that occurred only three hours after the Landers earthquake. The surface breaks show that the Landers' rupture involved four different faults and changed its strike between the southern and northern parts. In the southern part near the epicenter the surface faulting indicates a direction N10°W (Johnson Valley fault); while in the northern part (Camp Rock fault) the trend is N45°W. The focal mechanism deduced from body wave polarities gives an almost vertical strike slip with an azimuth N10°W corresponding to the direction of surface breaks in the epicentral region. The moment centroid determination indicates a strike slip earthquake with a strike azimuth of N20°W [*Kanamori et al., 1992*], an azimuth that is intermediate between the observed strike of the two primary fault segments observed in the field. In this paper we present a simple model, described by a small number of parameters, that produces farfield displacements very similar to the observations.

Paper number 92GL02822
0094-8534/93/92GL-02822$03.00

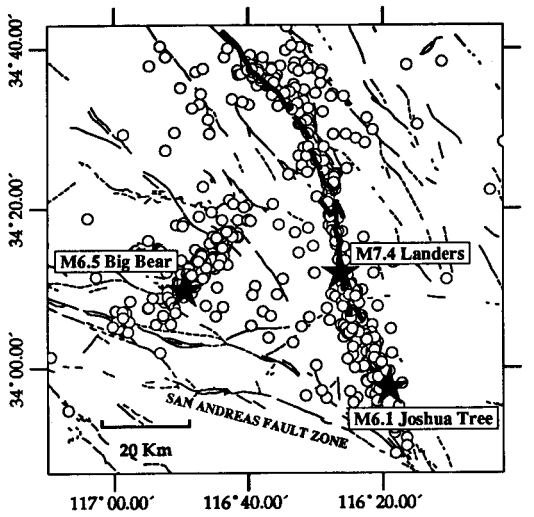

Fig. 1. Epicenters of the 1992 M 7.4 Landers and M_L 6.5 Big Bear earthquakes (stars) and their aftershocks (circles). Heavy solid lines represent the mapped surface ground rupture of the Landers earthquake (K. Sieh, Caltech, written communication, 1992). Earthquake epicenters courtesy of Jim Mori, U. S. Geological Survey, Pasadena. The aftershocks extend to the south of the observed surface breaks and into the region of the 22 April 1992 Joshua Tree M_L 6.1 earthquake.

The Landers earthquake was recorded regionally, on scale, by the accelerometric channels of the TERRAscope stations [*Kanamori et. al, 1991*]. We have used the accelerograms from the four closest stations SVD, PFO, GSC and PAS (Figure 2). The stations provide 180° azimuthal coverage of the faulting. The accelerograms are bandpassed between 40 s and 1.0 s then doubly integrated in the Fourier domain to obtain particle displacements. The synthetic displacements shown later were filtered in the same way.

FAULT MODEL

Using the preliminary epicenter 34.20°N,116.44°W and origin time 11:57:34 GMT from *Kanamori et al.* (1992) we found a systematic delay between observed and theoretical long-period waveforms. A careful look at the accelerometric records explained the discrepancy (Figure 3). The signals begin with a small emergent waveform followed about 3.5 seconds by a stronger arrival. Both of these arrivals are P waves because the S wave cannot arrive within this time interval given the distance between the stations and the epicenter. The delay between the two arrivals is not significantly different at the different stations. This indicates

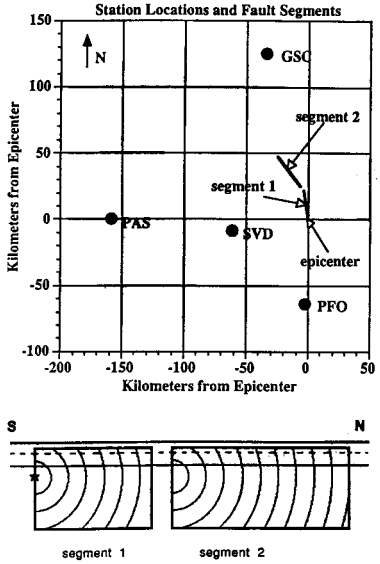

Fig. 2. (Upper Part) Map view of the TERRAscope station locations and the two fault segments. (Lower Part) Schematic cross-section of the two fault segments indicating the direction of rupture propagation and the position of the rupture front at different times. The horizontal lines parallel to the surface of the cross-sections show the positions of the velocity layers in the crustal models (Table 1 and text). The rupture front penetration into the upper layer gives rise to the strong Love waves observed in the data.

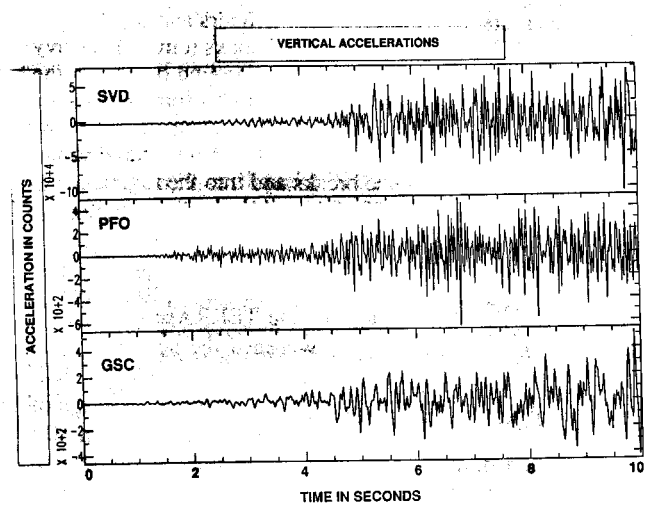

Fig. 3. The first 10 seconds of the vertical accelerograms at the three closest TERRAscope stations. The first arriving P wave from the mainshock arrives around 4.5 seconds. The preceding signal is due to a foreshock or increased seismic activity in the vicinity of the mainshock hypocenter.

that the origin of both the emergent and stronger arrivals have a similar epicenter but may differ in depth. We interpret this emergent arrival as the result of a foreshock in the epicentral region or of weak activity in the early beginnings of the rupture process. In the following computations we assumed that the origin time of the main shock is 11:57:37 GMT.

We assume that the surface offset gives an image of the actual fault at depth. Although the mapped surface rupture indicates that several segments were involved, the long-period data are primarily sensitive to only two segments. The existence of the two subevents can be seen in the North-South displacements recorded at stations SVD and PAS (Figure 4). These stations are located in a direction almost perpendicular to the average strike and are well situated to reveal the rupture complexity. They show very clearly the existence of two distinct pulses. This observation, associated with field observations, leads us to consider a model made from two distinct fault segments with different strike azimuths (Figure 2).

We have computed the displacements produced by the earthquake using a crustal model for Southern California

Modeling the long-period dynamic slip of the Landers mainshock we assume a dislocation process with two subevents. The fault is represented by an array of point sources. Each contribution is evaluated using a discrete wavenumber integration [*Bouchon, 1981*] associated with the reflection-transmission matrix technique [*Kennett, 1983*]. The first segment is modeled with a segment 20 km long extending N10°W from the epicenter. The second subevent is modeled with a segment 30 km long and oriented N40°W. The northern end of the first segment is offset from the southern end of the second segment by 3 km (Figure 2). The rupture plane extends from 1 to 15 km in depth.

The rupture initiates at a depth of 7 km beneath the epicenter and radially propagates unilaterally from this point at a constant rupture velocity of 3.0 km/s. The rupture velocity is well constrained by the widths of the pulses radiated by each subevent. There is a delay of one to two seconds between the time when the rupture ends on the first segment and begins on the second. This type of behavior for dynamic ruptures jumping from one segment to another is predicted in numerical simulations [*Harris et al., 1991*].

For each point on the fault the slip function is a ramp function with constant rise time and constant slip. The rise time and final slip are 4 s and 3.5 m for the first segment, respectively, and 4 s and 5.2 m for the second segment. The rise time is for a model that has constant slip everywhere on the fault plane. In this model the rise time controls the slope of the onset of the farfield displacement pulse. In a more complex model with heterogeneous slip, there will be a tradeoff between the rise time and the spatial variation of the slip [*Archuleta, 1984*]. More detailed resolution of the rise time will involve modeling particle velocity at higher frequencies.

We compare observed displacement time histories and synthetics computed using the crustal model (Table 1) at stations GSC, SVD, PFO and PAS (Model 1, Figure 4). The synthetics at SVD, the closest station, are in a good agreement with the observations, at least for the two horizontal components. Likewise the comparison is good for PAS where the fit is particularly satisfying when considering the structural heterogeneities encountered along the 165 km long path to Pasadena. The station PFO is located in the direction opposite to the direction of rupture propagation. Displacement amplitudes are therefore smaller than at SVD even though both are at nearly the same epicentral distance. At PFO there is no clear pulse to fit; the computation succeeds in the prediction of the amplitude and of the trend of the long period waveforms.

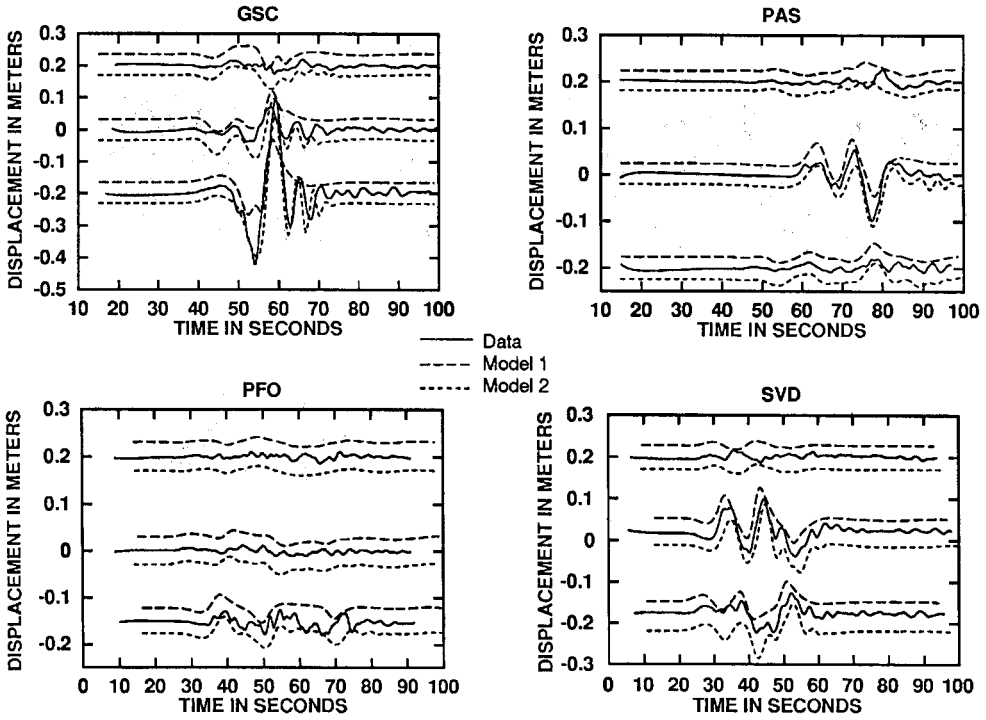

Fig. 4. Comparison of displacement time histories for data (solid line) and synthetics (dashed lines) computed for two crustal models. Time histories for the crustal model in Table 1 are shown as Model 1; the synthetics that include a lower velocity surface layer are shown as Model 2. For each station the upper trace is the vertical component of displacement, the middle is North-South and the bottom is East-West. Although there is general agreement between synthetics and data in the long period signature for Model 1, the synthetics do not agree with the shorter-period phases particularly prominent at GSC. The amplitude and phase are well matched throughout the time history for Model 2. The effect of the surficial layer on the generation of Love waves is especially evident at GSC.

[*Kanamori and Hadley, 1975*]. The crustal model consists of 3 layers over a half space (Table 1).

Table 1: Layered Crustal Structure in Southern California

Depth (km)	V_P (km/s)	V_S (km/s)	Density (kg/m^3)	Q_P	Q_S
0.0	5.50	3.20	2800	500	500
4.0	6.30	3.65	2900	500	500
26.0	6.80	3.90	3100	500	500
32.0	8.20	4.70	3200	500	500

We examined the possibility of a bilateral rupture on the first segment and found that the amplitudes at PFO are significantly overestimated in such a case.

The major discrepancy occurs at GSC. The large pulse observed on the EW component at GSC is followed by a series of oscillations that suggests dispersed surface waves. In this case they are Love waves. It is interesting to note that GSC is the only station showing such strong Love waves. GSC is located close to the direction of the rupture propagation. Our modeling indicates a high rupture velocity. The surface wave excitation will be strongly enhanced for a surficial rupture if rupture velocity is close to or greater than the shallow materials [*Bouchon, 1980*]. To verify this hypothesis we slightly changed the crustal model used in the computation by introducing a surficial lower velocity layer. In this second model the material properties of the first two kilometers of the model of Table 1 are changed to: V_P 4.1 km/s, V_S 2.3 km/s, density 2500 kg/m^3, Q_P 300 and Q_S 300.

Using the revised crustal structure we recomputed the synthetics (Model 2, Figure 4). Besides the change in the crustal structure we found that the delay in the time between the end of the rupture on the first segment and the initiation of rupture on the second segment was reduced to one second to better fit synthetics and data. The comparison between observed and synthetic seismograms for this new model is shown as Model 2 in Figure 4. With this second crustal structure we found an improved agreement between the observations and the synthetics for all three components of displacement on the four TERRAscope stations. The overall shape of the large pulse on the EW component at GSC is well predicted as well as the oscillations following the main pulse. The extra complexity in the observed waveforms appears to be a result of the surface waves generated by the rupture breaking the near-surface material. This is particularly clear when comparing the synthetic seismograms at SVD for Models 1 and 2 (Figure 4). These results illustrate that a realistic crustal model must include a lower-velocity surficial layer.

The seismic moment from our faulting model is 1.12×10^{20} N-m (1.12×10^{27} dyne-cm). The seismic moment derived from inversion of long-period surface waves is also 1.1×10^{20} N-m [*Kanamori et al., 1992*]. The coincidence of the seismic moment is exact in spite of the very different methodology used in both cases. Although the surface breaks are observed for about 70 km, we have used a faulting model with a total length of 53 km (including the 3 km jump between segments 1 and 2). This difference in total length is not

significant for the long-period moment release since the observed surface offsets vary along the strike but decrease near the ends. Allowing for 1.0 m of offset along an additional 20 km fault would contribute about 9.0×10^{18} N-m, or only about a 10% difference in the seismic moment. A moment magnitude **M** 7.4 is derived from $\log M_0 = 1.5\,\mathbf{M} + 16.0$ [*Hanks and Kanamori, 1979*]. (A discrepancy, M=7.3, arises if one uses $\mathbf{M} = 2/3 \log M_0 - 10.7$, because the quantity (2/3)16 is rounded before rounding the entire expression $(2/3)\times(\log M_0 - 16)$.)

DISCUSSION

A simple model of primarily unilateral propagation is consistent with the displacement time histories of the Landers earthquake. The model consists of rupture on two segments with different strikes: N10°W and N40°W. The two segments are 20 and 30 km long, respectively. The two subevents represent the large-scale complexity of the rupture. Although maps of the surface breaks show many discontinuous features, these features are not apparent in the displacement data. Our simple model gives a good fit to the data with only a few parameters. However, displacement data clearly require two distinct segments, each of which has its own continuous rupture. The smaller scale complexity observed in the surface breaks may be more evident in the higher frequency ground motion such as the particle velocity and acceleration time histories.

The excitation of surface waves is important to understand the amplitude of the displacement at regional distances. This is particularly critical in directions close to the rupture propagation where the high rupture velocity combined with directivity strongly affects the generation of Love waves in the surficial layers. The lower velocity surficial material was essential in our modeling of the long-period data.

The main rupture process itself seems to have been preceded for about 3 s by a weak seismic activity in the epicentral region, perhaps as a foreshock, a la the 1989 Loma Prieta, California, earthquake [*Wald et al., 1991*]. The rupture propagates unilaterally to the North with a high rupture velocity, about 3.0 km/s. The second event nucleates 8 s after the first; there is an arrest of the rupture of about 1 s between the breakage of the Johnson Valley fault and of the Camp Rock fault. The seismic moment of the subevents are 2.8×10^{19} N-m and 8.4×10^{19} N-m, leading to a total moment of 1.12×10^{19} N-m (M=7.4).

Acknowledgments. We are grateful to Hiroo Kanamori for providing the TERRAscope data. We appreciate Craig Nicholson's assistance with the data and Jean-Christophe Gariel's assistance with the numerical method. We thank Paul Spudich and an anonymous reviewers for their helpful comments. This work was supported by the UCSB Institute for Crustal Studies, the Southern California Earthquake Center and the Office of the Nuclear Regulatory Research, U. S. Nuclear Regulatory Commission Grant No. NRC-04-88-146 in cooperation with the French Commissariat à l'Energie Atomique.

REFERENCES

Archuleta, R. J. A faulting model for the 1979 Imperial Valley, California, earthquake, *J. Geophys. Res.*, **89**, 4559-4585, 1984.

Bouchon, M. The motion of the ground during an earthquake, Part I: the case of a strike-slip fault, *J. Geophys. Res.* **84**, 6149-6156, 1980.

Bouchon, M. A simple method to calculate Green's functions for elastic layered media, *Bull. Seismol. Soc. Am.* , **71**, 959-971, 1981.

Hanks, T. and H. Kanamori, A moment magnitude scale, *J. Geophys. Res.* , **84**, 6149-6156, 1979.

Harris, R. A, R. J. Archuleta and S. M. Day, *Geophys. Res. Lett.*, **18**, 893-896 (1991).

Kanamori, H., H. K. Thio, D. Dreger, E. Hauksson and T. Heaton, Investigation of the Landers, California, earthquake of 28 June 1992 using TERRAscope, *Geophys. Res. Lett.*, **19**, 2267-2270, 1992.

Kanamori, H., E. Hauksson, and T. Heaton, TERRAscope and CUBE project at Caltech, *EOS*, **72**, 564 (1991).

Kanamori, H. and D. Hadley. Crustal structure and temporal velocity change in Southern California,*Pure and Appl. Geophys.* **113**, 257-280, 1975.

Kennett, B. L. N. Seismic Wave Propagation in Stratified Media, Cambridge Univ. Press, Cambridge, 1983.

Wald, D. J., D. V. Helmberger and T. H. Heaton. Rupture model of the 1989 Loma Prieta earthquake from the inversion of strong-motion and broadband teleseismic data, *Bull. Seismol. Soc. Am.*, **81**, 1540-1572, 1991.

M. Campillo, LGIT/IRIGM, Université Joseph Fourier, BP 53X, 38041 Grenoble, France.

R. J. Archuleta, Institute for Crustal Studies, University of California, Santa Barbara, 93106-1100.

(Received: November 18, 1992;
Accepted: December 1, 1992.)